

# Conversion of Imine to Oxazole and Thiazole Linkages in Covalent Organic Frameworks

Peter J. Waller,<sup>†,§,‡,Ⓜ</sup> Yasmeen S. AlFaraj,<sup>†,‡</sup> Christian S. Diercks,<sup>†,§,‡,Ⓜ</sup> Nanette N. Jarenwattananon,<sup>†</sup> and Omar M. Yaghi<sup>\*,†,§,‡,Ⓜ,Ⓜ</sup>

<sup>†</sup>Department of Chemistry, University of California—Berkeley, Berkeley, California 94720, United States

<sup>‡</sup>Kavli Energy NanoSciences Institute at Berkeley, and Berkeley Global Science Institute, Berkeley, California 94720, United States

<sup>§</sup>Materials Sciences Division, Lawrence Berkeley National Laboratory, Berkeley, California 94720, United States

<sup>Ⓜ</sup>King Abdulaziz City for Science and Technology, Riyadh 11442, Saudi Arabia

## Supporting Information

**ABSTRACT:** Imine-linked ILCOF-1 based on 1,4-phenylenediamine and 1,3,6,8-tetrakis(4-formylphenyl)pyrene was converted through consecutive linker substitution and oxidative cyclization to two isostructural covalent organic frameworks (COFs), having thiazole and oxazole linkages. The completeness of the conversion was assessed by infrared and solid-state NMR spectroscopies, and the crystallinity of the COFs was confirmed by powder X-ray diffraction. Furthermore, the azole-linked COFs remain porous, as shown by nitrogen sorption experiments. The materials derived in this way demonstrate increased chemical stability, relative to the imine-linked starting material. This constitutes a facile method for accessing COFs and linkages that are otherwise difficult to crystallize due to their inherently limited microscopic reversibility.

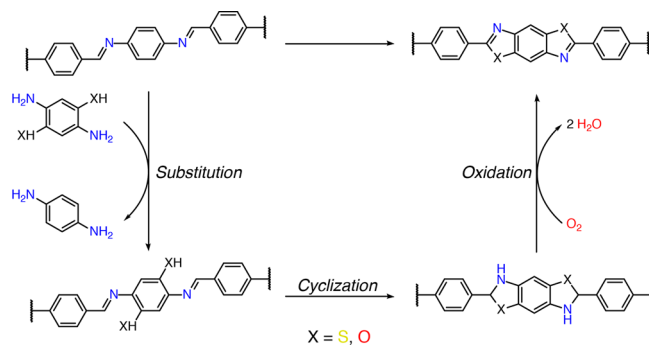
Covalent organic frameworks (COFs) are crystalline, porous networks, constructed from small molecular linkers connected through reversible bond formation.<sup>1–6</sup> It is this reversibility that not only leads to crystallinity through dynamic error correction during synthesis but also diminishes the resulting material's chemical stability. Recently, it has been shown that the dynamic nature of the bond also allows for the linkers of a COF to be exchanged postsynthetically, yielding an isostructural material with different pore metrics while retaining crystallinity.<sup>7,8</sup> In this work, we use the linkage's intrinsic reversibility to introduce linkers with functionalities incompatible with COF synthesis conditions. Notably, such functionalities cannot be added through established covalent postsynthetic modifications for COFs.<sup>9–14</sup> These functional groups then incite additional reactivity at the imine bond, resulting in multiple irreversible linking chemistries.

This signifies a method of bypassing the crystallization problem; typically, the development of linkages relies on serendipity in the optimization of reaction conditions that allow for sufficient reversibility to let crystallinity emerge.<sup>1,15–23</sup> Furthermore, this means that linkages with limited reversibility pose a particular challenge for the field. To circumvent this problem, our goal is to separate the crystallization from the final bond formation. As an example,

we recently demonstrated that imine-linked frameworks can be oxidized to form amide-bonded COFs that retain the structure of their progenitors.<sup>24</sup> Here, we take this approach a step further, showing that new functionalities can be incorporated into the framework by postsynthetic linker exchange, in order to bring about subsequent reactivity that leads to modified linkages.

For this study, we targeted linker exchanges using imine-bonded frameworks. These are an attractive starting point since they are the most abundant and well-studied COFs. In addition, the imine bond itself is poised for reaction giving rise to a wide array of chemical motifs. In this case, we aimed to form oxazole- and thiazole-linked frameworks by adding appropriately substituted linkers to the imine-based material after synthesis (Scheme 1). As a platform for this trans-

## Scheme 1. Proposed Strategy for Synthesis of Azole-Linked COFs through Substitution, Cyclization, and Oxidation

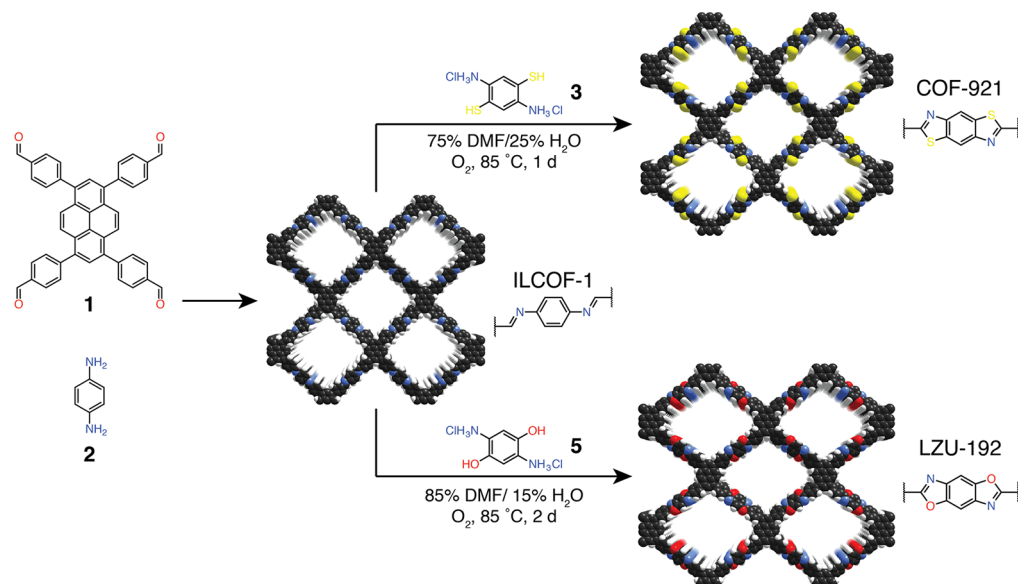


formation, we selected the previously reported ILCOF-1, a mesoporous, two-dimensional layered structure with **sql** topology (Scheme 2). The material was solvothermally synthesized using a modified literature procedure, wherein 1,3,6,8-tetrakis(4-formylphenyl)pyrene (**1**) and 1,4-phenylenediamine (**2**) were heated in a sealed tube at 120 °C for 4 days in a mixture of 1,2-dichlorobenzene, 1-butanol, and 6 M aqueous acetic acid solution.<sup>25</sup>

Received: June 3, 2018

Published: July 12, 2018

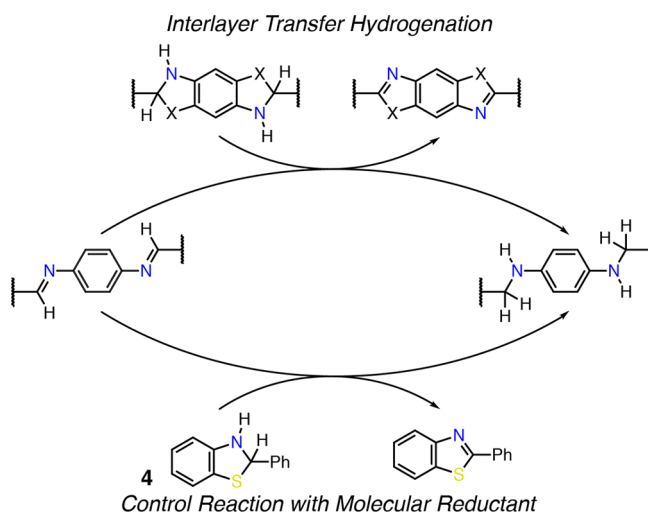
Scheme 2. Synthesis of Azole-Linked COF-921 and LZU-192 Materials from the Imine Precursor, ILCOF-1



With this material in hand, we began to investigate the exchange process by treating ILCOF-1 with 4 equiv of the functionalized linker. The synthesis of the new thiazole-linked COF, termed COF-921, was accessed through substitution of the 1,4-phenylenediamine linkers in ILCOF-1 with 2,5-diaminobenzene-1,4-dithiol dihydrochloride (3). As solvent, a mixture of DMF and water was used. During reaction optimization, it was shown that the presence of water provided better conversion of the imine functionality. This may be a result of faster imine hydrolysis and, therefore, more rapid linker exchange. In addition, literature reports suggest that water may assist in ring closure in the synthesis of azoles.<sup>26,27</sup> Addition of substantial amounts of water, however, lowered both crystallinity and surface area.

Since both molecular and amorphous polymeric benzothiazoles have been synthesized from aldehydes and amines using air as an oxidant, optimization was initially performed under ambient conditions.<sup>27,28</sup> Using these reaction conditions, the imine functionality was well-converted, as evidenced by both Fourier-transform infrared (FT-IR) and <sup>13</sup>C cross-polarization magic angle spinning (CP-MAS) NMR spectroscopy. However, unexpected signals appeared in the FT-IR spectrum at 1510 cm<sup>-1</sup> and in the <sup>13</sup>C NMR spectrum at 46 ppm (coincident with the spinning sidebands of the spectrum; see Supporting Information (SI) section S3). In order to explain these, we hypothesized a transfer hydrogenation side reaction, which serves to oxidize the intermediate dihydrothiazole linkages through the reduction of neighboring imines to amines (Scheme 3). Such a process would be consistent with the observation of both azole and amine functionalities in the material and would allow assignment of the carbon NMR signal as the benzylic carbon of the amine and the IR signal as arising from the amine moiety. To support this notion, the reaction between the molecular species 2-phenylbenzothiazoline (4) and imine-linked ILCOF-1 was studied. Others have shown that 4, when combined with Brønsted acids, is a powerful reductant of imines via transfer hydrogenation, so we anticipated it could be used in the synthesis of amine-linked material.<sup>29,30</sup> We found that treating ILCOF-1 with 4 in the presence of hydrochloric acid in DMF gave rise to a new

Scheme 3. Proposed Inter-COF Hydrogenation of Imine Linkages by Saturated Heterocycles, and Control Reaction with Molecular Reductant 4



material with the same signals in the FT-IR and solid state <sup>13</sup>C NMR. This corroborates our understanding that these signals are a result of benzylic amines formed during the course of the reaction.

In order to preclude the formation of the reduced side product, a variety of oxidants, including DDQ, *p*-chloranil, benzoquinone, and PhI(OAc)<sub>2</sub>, were applied, but their use resulted either in poor conversion or in loss of crystallinity. Ultimately, it was found that performing the reaction under an atmosphere of oxygen gave the desired product without structural degradation.

Additionally, we targeted the analogous oxazole-linked framework via linker exchange. In contrast to the thiazole case, where no such materials were previously reported, oxazole-linked COFs have been synthesized *de novo*.<sup>21,31</sup> In these cases, in order to obtain a crystalline material, the reaction conditions required substantial modification from those employed in typical imine COF syntheses. Our approach, instead, relies on easily crystallized imine frame-

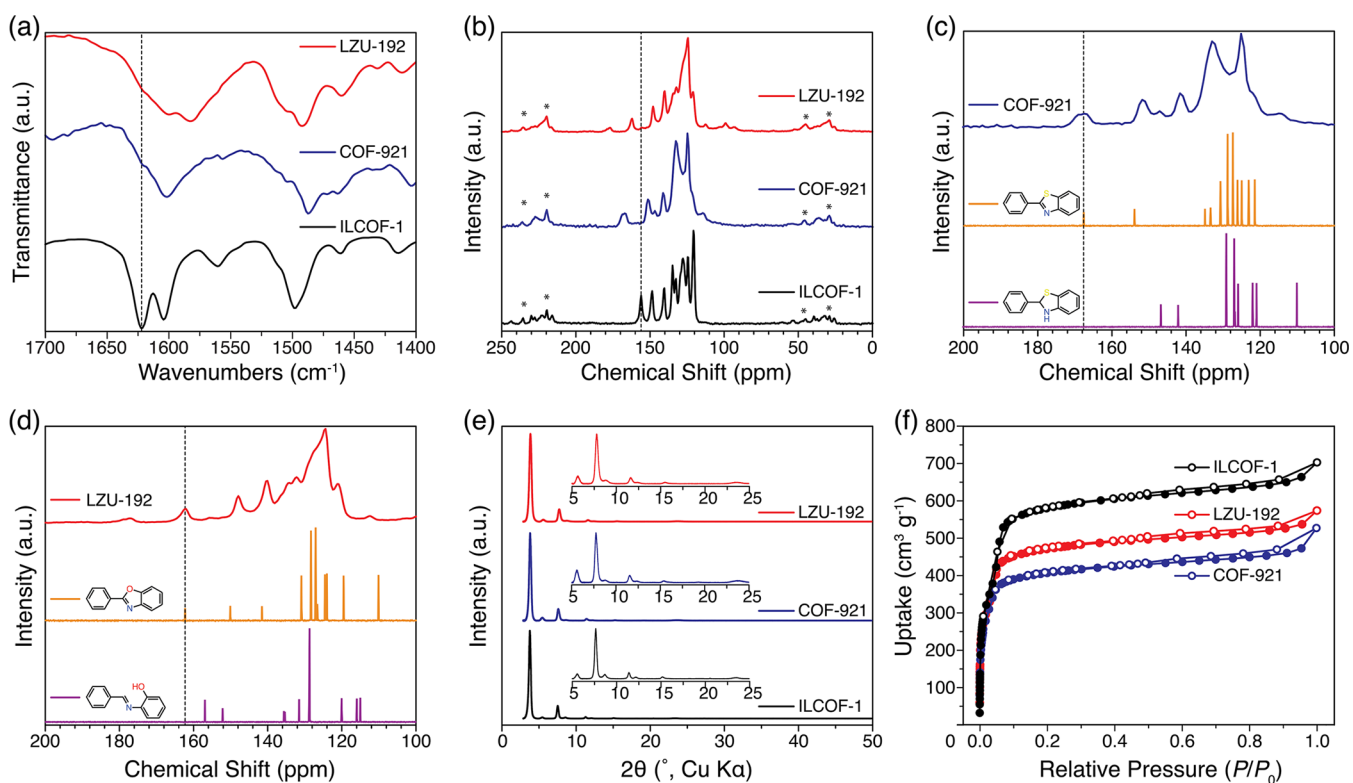


**Figure 1.** (a) FT-IR spectra of the COFs under investigation, with diagnostic imine stretch indicated. (b)  $^{13}\text{C}$  CP-MAS NMR spectra of the imine-linked starting material and the two azole-linked products, with iminyl carbon signal highlighted. Spinning sidebands are denoted with asterisks. (c) Comparison of liquid-state  $^{13}\text{C}$  NMR spectra of benzothiazole model, unoxidized benzothiazoline, and the  $^{13}\text{C}$  CP-MAS NMR spectrum of COF-921. (d) Comparison of liquid-state  $^{13}\text{C}$  NMR spectra of hydroxyl-substituted imine, benzoxazole, and the solid-state NMR spectrum of LZU-192. (e) PXRD patterns of these materials, showing retention of crystallinity. (f) Nitrogen sorption isotherms, performed at 77 K, showing permanent porosity of all materials. Solid and open circles indicate adsorption and desorption, respectively. Uptake is defined as cubic centimeters of  $\text{N}_2$  at 1 atm and 0  $^\circ\text{C}$  per gram of COF sample.

works as bases for subsequent exchange and modification. The synthesis of oxazole-linked material from ILCOF-1 produces the previously reported LZU-192.<sup>31</sup> The conversion was performed using 2,5-diaminohydroquinone dihydrochloride (**5**, Scheme 2) as the new linker. As in the previous case, under air the imine was well-converted, but a side product with the same FT-IR and  $^{13}\text{C}$  NMR spectral features was evident. The material was converted to the desired product by allowing the reaction to proceed under oxygen, though FT-IR indicates a small amount of this side product may be present.

Conversion of the material to the desired azoles was spectroscopically verified in two ways. The first indication of conversion was the attenuation of the imine stretch in the FT-IR spectra ( $1622\text{ cm}^{-1}$ , Figure 1a). In the case of COF-921, a small amount of residual intensity remains at  $1622\text{ cm}^{-1}$ , implying that a minute amount of the imine linkage may still exist, perhaps at inaccessible defect sites. On the other hand, while the FT-IR spectrum of LZU-192 shows broad intensity in this region, at least some of this can be assigned to the expected vibrations of the oxazole ring.<sup>32,33</sup>

In addition, affirmative indications of conversion are provided by FT-IR spectroscopy. For COF-921, the benzothiazole ring's breathing ( $962\text{ cm}^{-1}$ ) mode is present in the spectrum, implying formation of the desired product.<sup>34</sup> In the spectrum of LZU-192, the benzoxazole ring modes ( $1590$  and  $1056\text{ cm}^{-1}$ ) are observed, further supporting synthesis of the product (SI, section S4).<sup>32,33</sup>

These compounds were also characterized using  $^{13}\text{C}$  CP-MAS NMR spectroscopy (Figure 1b). In the converted materials, the peak corresponding to the imine carbon ( $156\text{ ppm}$ ) is attenuated. In turn, it is replaced by new resonances at  $167\text{ ppm}$  for the thiazole and  $163\text{ ppm}$  for the oxazole. The assignment of these signals to C2 of the azoles was confirmed by comparison to molecular models (Figure 1c,d). Given the difficulty normally encountered in accomplishing the oxidative cyclization of the hydroxy-substituted imine compound, LZU-192 was also contrasted against the uncyclized model to verify that oxidative cyclization took place (Figure 1d).

The structure of the materials was examined using powder X-ray diffraction (Figure 1e). Notably, the crystallinity of the imine COF was preserved and all were assigned to the same space group (*Pmnm*, No. 59), implying that the overall symmetry of the material is maintained. Importantly, the unit cell parameters do change during the transformation from ILCOF-1 ( $a = 30.9\text{ \AA}$ ,  $b = 32.5\text{ \AA}$ ,  $c = 3.7\text{ \AA}$ ) to COF-921 ( $a = 34.1\text{ \AA}$ ,  $b = 32.5\text{ \AA}$ ,  $c = 3.6\text{ \AA}$ ) and LZU-192 ( $a = 33.0\text{ \AA}$ ,  $b = 31.0\text{ \AA}$ ,  $c = 3.6\text{ \AA}$ ). Therefore, while the unit cell parameters do change, the material's overall structure remains the same.

The porosity of the COFs was examined through nitrogen sorption experiments (Figure 1f). The benzothiazole- and benzoxazole-functionalized materials have surface areas of  $1550$  and  $1770\text{ m}^2\text{ g}^{-1}$ , respectively, versus a surface area of  $2050\text{ m}^2\text{ g}^{-1}$  for the imine. This represents a loss of 24% for COF-921 and 14% for LZU-192 versus ILCOF-1. A lower gravimetric surface area is expected for the converted materials,

since their crystallographic densities are higher (SI section S5). However, the observed surface area loss is greater than expected. We hypothesize that, during the exchange, the imine starting materials may undergo hydrolysis, resulting in the formation of insoluble oligomers that may block the pores, or alternatively, the linker may become trapped in the pores. In spite of this, the oxazole material has a higher surface area than that of any currently known oxazole COFs.

In order to probe our hypothesis regarding the irreversibility of the azole linkages relative to the imine, chemical stability tests were performed. The materials were submerged in basic (10 M NaOH) and acidic (12.1 M HCl, 18 M H<sub>2</sub>SO<sub>4</sub>, 14.8 M H<sub>3</sub>PO<sub>4</sub>, and 9 M H<sub>2</sub>SO<sub>4</sub> in DMSO) solutions for 1 d, and subsequently analyzed by PXRD and FT-IR (SI section S12). Interestingly, all materials, even the imine-linked ILCOF-1, proved stable in HCl. However, the PXRD patterns of imine-linked ILCOF-1 treated with solutions containing H<sub>2</sub>SO<sub>4</sub> showed the emergence of a new phase. Furthermore, the FT-IR spectra indicated that a large amount of imine hydrolysis had occurred in the solutions of NaOH, H<sub>2</sub>SO<sub>4</sub>, and H<sub>3</sub>PO<sub>4</sub>, as evidenced by the attenuation of the imine signal, and growth of the aldehyde peak. In contrast, the azole materials performed well in all conditions, where no changes in the PXRD pattern, and only minimal changes in the FT-IR spectra, were observed. This serves as strong evidence for the increased irreversibility of the azole linkages and shows that this technique is capable of producing chemically stable materials.

We demonstrated the utility of a method based on substitution followed by oxidative cyclization in producing new COFs of new linkages. This method is promising in advancing COF chemistry from the usual reversible linkages to more desirable and difficult to make linkages of limited reversibility. The high crystallinity and porosity of these materials are a testament to the value of this method, which translates the quality of the imine precursor to more irreversible chemistries.

## ■ ASSOCIATED CONTENT

### Supporting Information

The Supporting Information is available free of charge on the ACS Publications website at DOI: 10.1021/jacs.8b05830.

Methods and additional data (PDF)

## ■ AUTHOR INFORMATION

### Corresponding Author

\*yaghi@berkeley.edu

### ORCID

Peter J. Waller: 0000-0002-4013-8827

Christian S. Diercks: 0000-0002-7813-0302

Omar M. Yaghi: 0000-0002-5611-3325

### Notes

The authors declare no competing financial interest.

## ■ ACKNOWLEDGMENTS

This work was supported by the Army Research Office through a Multidisciplinary University Research Initiatives (MURI) Award through Grant WG11NF-15-1-0047. P.J.W. additionally thanks the NSF and the Berkeley Center for Green Chemistry for support via the Systems Approach to Green Energy Integrative Graduate Education and Research Traineeship

(1144885). Y.S.F. is supported by the Gifted Student Program Scholarship through the King Abdullah University of Science and Technology. C.S.D. acknowledges funding through a Kavli ENSI Philomathia Graduate Student Fellowship. The authors thank Dr. Chenfei Zhao, Mary E. Garner and Robinson W. Flaig for helpful discussions.

## ■ REFERENCES

- (1) Côté, A. P.; Benin, A. I.; Ockwig, N. W.; O’Keeffe, M.; Matzger, A. J.; Yaghi, O. M. *Science* **2005**, *310* (5751), 1166–1170.
- (2) El-Kaderi, H. M.; Hunt, J. R.; Mendoza-Cortés, J. L.; Côté, A. P.; Taylor, R. E.; O’Keeffe, M.; Yaghi, O. M. *Science* **2007**, *316* (5822), 268–272.
- (3) Feng, X.; Ding, X.; Jiang, D. *Chem. Soc. Rev.* **2012**, *41* (18), 6010–6022.
- (4) Ding, S.-Y.; Wang, W. *Chem. Soc. Rev.* **2013**, *42* (2), 548–568.
- (5) Waller, P. J.; Gándara, F.; Yaghi, O. M. *Acc. Chem. Res.* **2015**, *48* (12), 3053–3063.
- (6) Diercks, C. S.; Yaghi, O. M. *Science* **2017**, *355* (6328), eaal1585.
- (7) Qian, C.; Qi, Q.-Y.; Jiang, G.-F.; Cui, F.-Z.; Tian, Y.; Zhao, X. J. *Am. Chem. Soc.* **2017**, *139* (19), 6736–6743.
- (8) Zhang, G.; Tsujimoto, M.; Packwood, D.; Duong, N. T.; Nishiyama, Y.; Kadota, K.; Kitagawa, S.; Horike, S. *J. Am. Chem. Soc.* **2018**, *140* (7), 2602–2609.
- (9) Huang, N.; Krishna, R.; Jiang, D. *J. Am. Chem. Soc.* **2015**, *137* (22), 7079–7082.
- (10) Ding, S.-Y.; Gao, J.; Wang, Q.; Zhang, Y.; Song, W.-G.; Su, C.-Y.; Wang, W. *J. Am. Chem. Soc.* **2011**, *133* (49), 19816–19822.
- (11) Lohse, M. S.; Stassin, T.; Naudin, G.; Wuttke, S.; Ameloot, R.; De Vos, D.; Medina, D. D.; Bein, T. *Chem. Mater.* **2016**, *28* (2), 626–631.
- (12) Huang, N.; Chen, X.; Krishna, R.; Jiang, D. *Angew. Chem., Int. Ed.* **2015**, *54* (10), 2986–2990.
- (13) Meri-Bofi, L.; Royuela, S.; Zamora, F.; Ruiz-Gonzalez, M. L.; Segura, J. L.; Muñoz-Olivas, R.; Mancheño, M. J. *J. Mater. Chem. A* **2017**, *5* (34), 17973–17981.
- (14) Sun, Q.; Aguila, B.; Perman, J.; Earl, L. D.; Abney, C. W.; Cheng, Y.; Wei, H.; Nguyen, N.; Wojtas, L.; Ma, S. *J. Am. Chem. Soc.* **2017**, *139* (7), 2786–2793.
- (15) Kuhn, P.; Antonietti, M.; Thomas, A. *Angew. Chem., Int. Ed.* **2008**, *47* (18), 3450–3453.
- (16) Uribe-Romo, F. J.; Hunt, J. R.; Furukawa, H.; Klöck, C.; O’Keeffe, M.; Yaghi, O. M. *J. Am. Chem. Soc.* **2009**, *131* (13), 4570–4571.
- (17) Jackson, K. T.; Reich, T. E.; El-Kaderi, H. M. *Chem. Commun.* **2012**, *48* (70), 8823–8825.
- (18) Guo, J.; Xu, Y.; Jin, S.; Chen, L.; Kaji, T.; Honsho, Y.; Addicoat, M. A.; Kim, J.; Saeki, A.; Ihee, H.; Seki, S.; Irle, S.; Hiramoto, M.; Gao, J.; Jiang, D. *Nat. Commun.* **2013**, *4*, 2736.
- (19) Fang, Q.; Zhuang, Z.; Gu, S.; Kaspar, R. B.; Zheng, J.; Wang, J.; Qiu, S.; Yan, Y. *Nat. Commun.* **2014**, *5*, 4503.
- (20) Zhuang, X.; Zhao, W.; Zhang, F.; Cao, Y.; Liu, F.; Bi, S.; Feng, X. *Polym. Chem.* **2016**, *7* (25), 4176–4181.
- (21) Pyles, D. A.; Crowe, J. W.; Baldwin, L. A.; McGrier, P. L. *ACS Macro Lett.* **2016**, *5* (9), 1055–1058.
- (22) Deblase, C. R.; Dichtel, W. R. *Macromolecules* **2016**, *49* (15), 5297–5305.
- (23) Jin, E.; Asada, M.; Xu, Q.; Dalapati, S.; Addicoat, M. A.; Brady, M. A.; Xu, H.; Nakamura, T.; Heine, T.; Chen, Q.; Jiang, D. *Science* **2017**, *357* (6352), 673–676.
- (24) Waller, P. J.; Lyle, S. J.; Osborn Popp, T. M.; Diercks, C. S.; Reimer, J. A.; Yaghi, O. M. *J. Am. Chem. Soc.* **2016**, *138* (48), 15519–15522.
- (25) Rabbani, M. G.; Sekizkardes, A. K.; Kahveci, Z.; Reich, T. E.; Ding, R.; El-Kaderi, H. M. *Chem. - Eur. J.* **2013**, *19* (10), 3324–3328.
- (26) Lee, Y.-S.; Cho, Y.-H.; Lee, S.; Bin, J.-K.; Yang, J.; Chae, G.; Cheon, C.-H. *Tetrahedron* **2015**, *71* (4), 532–538.

- (27) Bala, M.; Verma, P. K.; Sharma, D.; Kumar, N.; Singh, B. *Mol. Diversity* **2015**, *19* (2), 263–272.
- (28) Rabbani, M. G.; Islamoglu, T.; El-Kaderi, H. M. *J. Mater. Chem. A* **2017**, *5* (1), 258–265.
- (29) Zhu, C.; Akiyama, T. *Org. Lett.* **2009**, *11* (18), 4180–4183.
- (30) Zhu, C.; Akiyama, T. *Adv. Synth. Catal.* **2010**, *352* (11–12), 1846–1850.
- (31) Wei, P.-F.; Qi, M.-Z.; Wang, Z.-P.; Ding, S.-Y.; Yu, W.; Liu, Q.; Wang, L.-K.; Wang, H.-Z.; An, W.-K.; Wang, W. *J. Am. Chem. Soc.* **2018**, *140* (13), 4623–4631.
- (32) Bassignana, P.; Cogrossi, C.; Gandino, M. *Spectrochim. Acta* **1963**, *19* (11), 1885–1897.
- (33) Tullos, G. L.; Powers, J. M.; Jeskey, S. J.; Mathias, L. J. *Macromolecules* **1999**, *32* (11), 3598–3612.
- (34) Tan, N.; Xiao, G.; Yan, D. *Chem. Mater.* **2010**, *22* (3), 1022–1031.